An approach for multisensor harmonization in snow cover area mapping

Rune Solberg and Hans Koren
Norwegian Computing Center (NR)
Oslo, Norway
rune.solberg@nr.no

Eirik Malnes, Jörg Haarpaintner, Inge Lauknes
NORUT IT
Tromsø, Norway
eirik.malnes@itek.norut.no

Abstract— **In this study, we have developed an approach for fusion of optical and SAR data for snow cover fraction (SCF) retrieval that avoids the typical blending effects when combining independently retrieved geophysical data from different sensors. Instead of undertaking the sensor fusion at the geophysical parameter level, the fusion is done at the electromagnetic signal level. A state model, based on Hidden Markov Model theory, has been developed for the simultaneous signal from the optical and the SAR sensors. The model goes through a given set of states through the snowmelt season where transition probability distribution functions of time have been determined for each state transition. A coupling between corresponding models for optical and SAR observations has been developed in order to make a more reliable model of the sensor co-variation.**

Snow cover area, multisensor, SAR, optical, Hidden Markov Model.

I. INTRODUCTION

The snow cover has a substantial impact on the interaction processes between the atmosphere and the surface, thus the knowledge of snow variables is important in climatology, weather forecasting, and hydrology. In mountainous areas and in the northern Europe, snowfall is a substantial part of the overall precipitation. In order to perform sustainable management of water, in particular for hydropower production and flood protection, information on the snow cover is mandatory.

The latest generation of optical and SAR sensors has opened for multi-sensor time-series mapping of snow cover. A few algorithms for this have been published. Raggam, Almer and Strobel demonstrated in [7] how snow cover retrieved from multi-parameter airborne SAR and SPOT HRV can be combined. Koskinen et al. analyzed a time series of NOAA AVHRR and ERS-2 SAR images in [2]. However, they did no actual combination of the two other than studying how the snow cover developed as observed by the two sensors. Tait et al. developed a true combination of data from two sensors to produce a snow map in [11]. NOAA AVHRR data and SSM/I data were analyzed together with climate station data and a digital terrain model in a decision tree in order to produce continental-scale snow maps for North America.

The lack of access to frequent acquisitions of both SAR and optical data changed with the launches of Radarsat and ENVISAT (with ASAR) that in wide swath modes are able to deliver data of frequent coverage for a given geographical area.

This allowed multi-sensor fusion with AVHRR and MODIS on a frequent basis. Examples of such fusion can be found in [9] and [10]. The optimal situation is when optical and SAR sensors are on the same platform, which ensures acquisitions under exactly same conditions. The only satellite platform delivering such data currently is ENVISAT. ASAR and MERIS can be acquired simultaneously. However, cloud detection is not possible with MERIS, and the alternative sensor AATSR has a much smaller swath. So this gives no practical/operational solution to the problem. Anyway, an example of using AATSR for detecting clouds in a partial MERIS scene can be found in [12]. An example of the use of ASAR and MERIS in combination can also be found in [10].

II. OVERALL METHODOLOGICAL IDEA

A serious challenge of multi-sensor fusion algorithms is that the optical and SAR sensors measure different physical phenomena. The effects from photon scattering, transmission and absorption near the snow surface at the snow-grain-size level dominate the optical snow spectrum. The radar signal is dominated by effects due to dielectric properties of the snow medium as well as snow surface roughness (for wet snow) or a combination of the snow pack structure and the ground below. In addition come contributions from the bare ground surface for fractional snow cover conditions. When blending snow cover fraction (SCF) retrieved from these two types of sensors into a fractional snow cover product, heterogeneities will easily appear as shown in the example in Figure 1, which is based on the algorithm in [9]. This is a problem in several applications. Variability in the retrieved parameter that is not related to the true SCF may create wrong interpretations when the snow cover is used as an indicator for climate change or as a variable in a hydrological model.

In this study, we have developed an approach avoiding the blending effects. Instead of undertaking the sensor fusion at the geophysical parameter level (where SCF has been retrieved independently from the optical and SAR sensors), the fusion is done at the electromagnetic signal level. A state model, based on Hidden Markov Model theory, has been developed for the simultaneous signal from the optical and the SAR sensors. The model goes through a given set of states through the snowmelt season where transition probability distribution functions of time have been determined for each state transition. A coupling between models for optical and SAR observations has been developed in order to make more reliable co-variation.
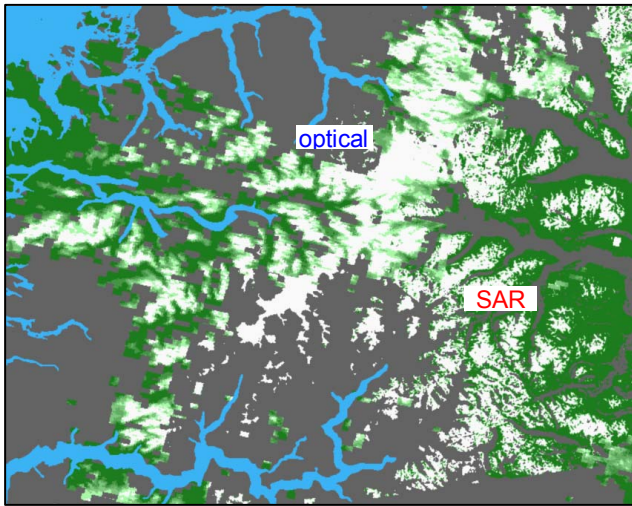
Figure 1. An example of a multi-sensor product where blended optical and SAR observations give somewhat different results. The lower right part of the map has SAR as sensor source. The SCF retrieved from SAR is more "granular" or binary than the results from optical data

III. SINGLE SENSOR RETRIEVAL ALGORITHMS

The interpretation of the optical and SAR signals with respect to snow cover fraction is based on existing retrieval algorithms that have been tested and refined over many years.

A. Optical retrieval algorithm

The optical SCF algorithm is based on an empirical reflectance-to-snow-cover model originally proposed for NOAA AVHRR [1] and later refined [8]. The algorithm has recently been tailored to MODIS data by NR. It retrieves the snow cover fraction for each pixel. The model is calibrated by providing two points of a linear function relating observed reflectance (or radiance) to snow cover fraction. The calibration is done automatically by means of calibration sites. Statistics from the sites are then used to compute calibration values determining the linear relationship.

A particular problem for practical use of the algorithm is clouds. NR has experimented with several approaches, and the current best cloud detection algorithm is based on K Nearest Neighbor (KNN) classification of MODIS data. In a KNN classifier a pixel, represented by a vector of band values, is assigned a label, which is the most prevalent label among the K nearest labeled vectors in a reference set. A KNN classifier is an asymptotically optimum (maximum likelihood) classifier as the size of the reference set increases.

B. SAR retrieval algorithm

Several papers have demonstrated the capability of SAR for wet snow mapping using ERS and Radarsat standard modes (see, e.g., [5] and [2]). Wet snow was detected by utilizing the high absorption, and therefore low backscatter, of wet snow and then comparing the backscatter with a corresponding pixel in a reference image acquired during dry-snow or snow-free conditions. Present algorithms use a -3 decibel (dB) threshold to discriminate between wet snow and dry snow/bare ground.

A more fine-tuned and variable threshold might be applied if the vegetation cover is known.

Recently, dry snow has also been inferred by using a 20 × 20 km² moving window and a digital elevation model (DEM). Dry snow is postulated above the mean wet snow elevation zone within the moving window [3]. The methodology has been further improved by taking into account in situ air temperature measurements from the meteorological stations, that are applied for deriving an interpolated temperature map based on standard 6ºC per km height-laps rate and a DEM [4].

IV. TIME SERIES STUDY

A study of the temporal development of optical and SAR observations of snow throughout a snowmelt season is presented below.

A. Data set

The study was carried out using data from the Heimdalen-Valdresflya test site in the Jotunheimen mountain region in the central part of southern Norway (9.0° E; 61.4° N). The site is of about 200 km² with an elevation range of 1050 to 1840 m a.s.l. The area is free of tall vegetation except for some birch in the lowest locations.

A time series of Terra MODIS and ENVISAT ASAR data was acquired for the period 15 April until 29 July 2005. For ASAR we used all available wide-swath images of VV-polarization.

The MODIS data were processed by the retrieval algorithm described in the previous section. The Snow Cover Fraction (SCF) values presented in the study below are close to reflectance values of the study site (which is the reason that both are not presented). For SAR, relative (differential) backscatter values have been used in the study. They have been calculated by computing the ratio of snow observations to observations of the dry snow pack of the same acquisition mode and geometry (as a substitute to snow-free acquisitions during the summer).

Air temperature data have been recorded at two elevations close to the test site (Bitihorn at 1607 m.a.s.l. and Bygdin at 1060 m.a.s.l.). Under normal conditions the air temperature in the test site will be close to the mean value of the temperatures at these sites. Precipitation data have been measured slightly farther away by meteorological stations at Beito (754 m.a.s.l., 15 km to the south) and Skåbu (890 m.a.s.l., 36 km north-east of the test site). Data from these stations provide indications of days with precipitation in the test area. Some fieldwork was also carried out in the period.

Figure 2 illustrates a part of the data set, which is the basis of the discussion below, with optical and SAR observations, and air temperatures and precipitation. Optical and SAR observations are mean values from a flat area of 2 km² at approximately 1350 m.a.s.l.

B. Results

1) Comments to optical observations: The retrieved SCF is close to 100% until about 10 June. Most probably the area is
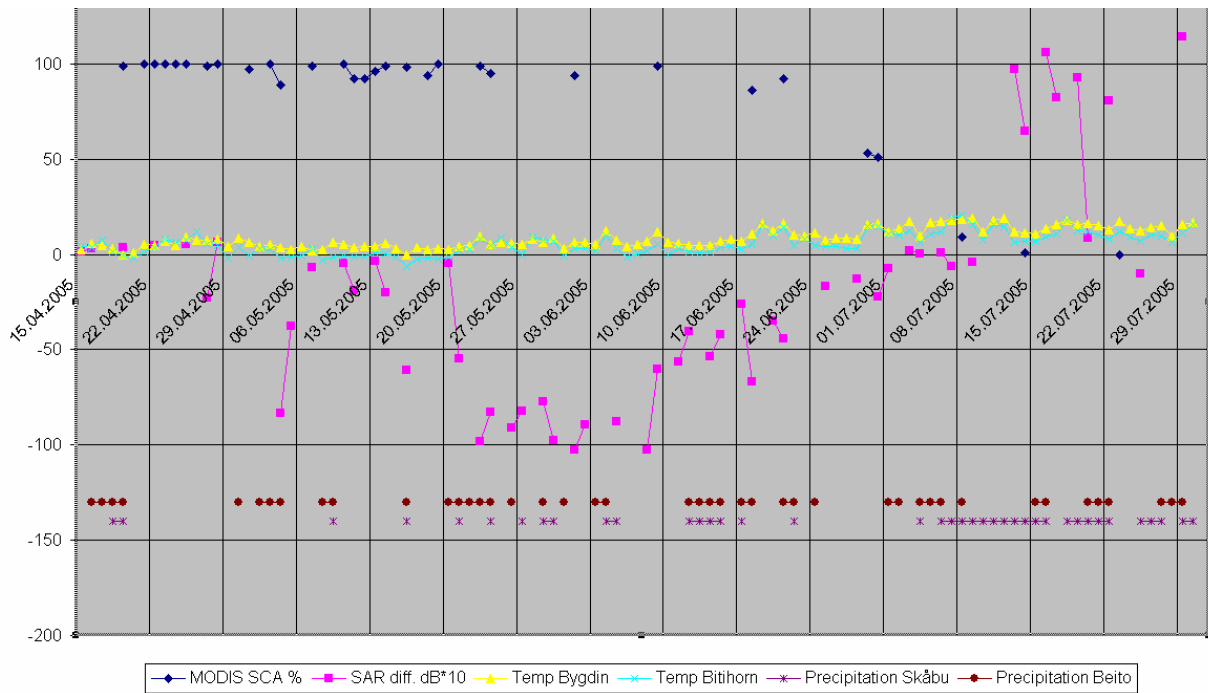
Figure 2. Optical and SAR observations shown together with air temperature and precipitation measurements throughout the snowmelt season of 2005 in a section of the Heimdalen-Valdresflya test site in south Norway

completely covered with snow until this date. From then on the SCF is reduced, first slowly and then rapidly down to 0% at around 15 July.

The air temperature is probably above zero in daytime in the last part of April, but it is cold in the nights and the weather is fine. Such conditions will keep the snow dry and any melting will take place by sublimation.

In the period 1-20 May, the mean day temperature is below zero, and there are some days with snowfall. For some days the retrieved SCF is below 100%. A closer look at the MODIS images for these days shows that retrieved SCF probably is erroneous due to undetected clouds at some calibration sites applied by the retrieval algorithm.

From 20 May until 17 June, the temperatures go up and down. The snow is probably wet, and melting has started. There are many days with precipitation, but the SCA is not much affected. For the last week there are no MODIS observations due to cloud cover.

After 17 June the temperature increases and the melting accelerates. Around 15 July there is no snow left in the area.

2)   Comments to SAR observations: The general behavior of the differential backscattering coefficient as a function of time can be grouped into 4-5 phases:

a. The difference is close to zero before the end of April. This corresponds to dry snow cover.

b. After this date there are several events where the surface layer of the snow becomes wet (due to positive average temperatures) resulting in low backscatter. This seems in general to be consistent with high daytime temperatures resulting in snowmelt in the top layer.

c. From May 20 to June 10, the backscatter difference drops several decibels. This is consistent with sustained high mean temperatures resulting in gradually wetter snow surface. The minimum difference is around June 10. We interpret this minimum as the snow pack being saturated by liquid water.

d. Snow melting from now on accelerates. This is consistent with the MODIS-derived snow cover fraction, where the SCF now suddenly starts to decrease. The decrease correlates well with an increase in the backscatter difference from June 10 to July 15.

e. After July 15 the snow cover fraction is close to zero. The relatively large variations in backscatter differences in the period between July 15 and August 1 can be explained partially by the selection of reference SAR images. Our main choice of reference data is from the wintertime when most of the rocks and surface roughness is partially smoothed by the snow cover. Exposed rocks in the summer images probably explain why there can be observed differences as high as 5 dB. Also, the bare soil may have variable soil moisture, leading to variable backscattering [13].

V.   OUTLINING THE NEW APPROACH

A. The general temporal development of the snow

The typical temporal development of optical and SAR observations of snow from winter to summer seasons goes through specific stages, as indicated in the previous section.
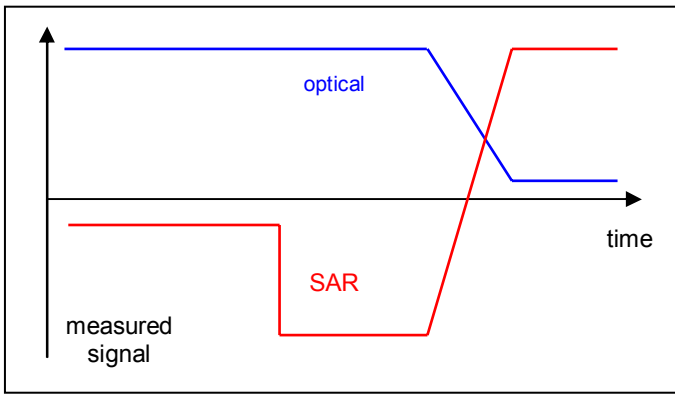
Figure 3. The typical stages of the snow as observed with optical and SAR sensors. For optical, the signal would normally be reflectance or radiance. The SAR signal illustration is based on differential backscatter

For optical observations, there are three stages: Winter situation with full snow coverage, snow-cover depletion period, when bare ground gradually appears and covers a larger fraction of the pixel, and finally the last stage with only snow-free ground. The three stages are outlined in Figure 3. Some small deviations from the trends were observed, mainly due to misinterpretation of clouds. Snowstorm events may also create deviations. However, the observed deviations are of a rather small magnitude.

SAR goes through the same stages as the optical data, but with an additional stage. The winter season stage is dominated by the ground backscatter. When the snowmelt starts, the snow surface turns wet and the backscatter is significantly reduced. This stage is then followed by a stage of gradual increase in the area fraction of snow-free ground in each pixel – the snow-cover depletion stage. The backscatter is increasing correspondingly. The final stage, completely snow-free ground, is characterized by high backscatter. The stages are illustrated in Figure 3.

As was clearly illustrated in the previous section, the variability of the differential SAR backscatter within each stage is very much higher than the variability of the reflectance within the corresponding stages. The SAR is very sensitive to presence of surface water. Wet precipitation after a cold period, as rain or sleet, or higher temperatures melting the surface layer, will immediately change the backscatter from being dominated by ground backscatter to backscatter entirely from the snow surface. Precipitation is typically frequent in mountain regions. Therefore, the early snowmelt period with temperatures flipping around zero will typically create large variability in the backscatter according to where in the ground/snow-pack/snow-surface package most of the backscattering is taking place. This variability is reduced, as the snow pack turns almost saturated by water in the later part of the snowmelt season. However, when e.g. rocks start to appear above the snow surface, the backscatter increases significantly. Since the ground surface roughness will dominate as gradually more bare ground appears, and the terrain roughness seldom is homogeneous and isotropic, there might not be any simple relationship between the snow-cover fraction and the differential backscatter level for a pixel.
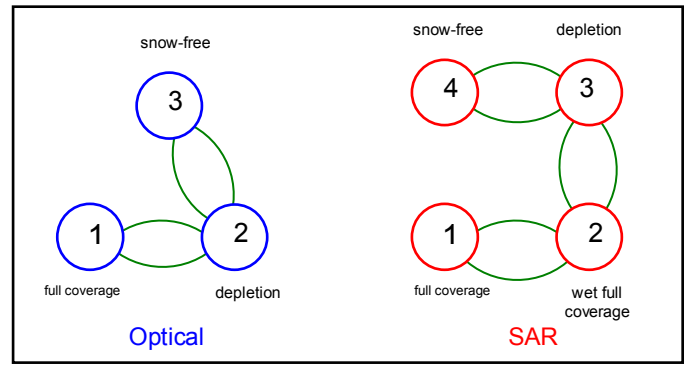

Figure 4. State diagram for SAR and optical observations based on the stages illustrated in Figure 3

It should also be noticed that the difference of the general backscatter levels between the winter season and the summer season depends on the selection of reference images for the backscatter ratio. Most images used here are from the winter season. The SAR will then penetrate somewhat into the frozen ground, which will give a somewhat different backscatter than a rather wet ground surface in the summer. There will also be some contribution from the snow pack, in particular if ice layers (crust) are present in the snow pack.

B.   A state model for the snow development

The stages outlined in the subsection above might be applied as valuable information in a multi-sensor model for retrieval of snow cover fraction in the spring season. The stages determine corresponding regimes for the interpretation of the reflectance and backscatter signals. In particular for the interpretation of the SAR signal where retrieving the SCF from a single observation is rather dangerous. The stages might be used to impose particular interpretational restrictions in the model. With data from two independent sources, SAR and optical, snow cover fraction retrieval can be made more robust. In particular when using optical observations to determine the current SAR observation stage and, thereby, setting a corresponding interpretation regime for backscatter signal. This would in particular be crucial for stage-to-stage transition decisions.

The staging, ordering of (or relationships between) stages and the fact that the various stages have special characteristics (in particular interpretation restrictions), suggest that a multi-sensor model could be based on general state model. There is quite a lot of theory developed for such models, called Finite State Automata (FSA) or Finite State Machines (FSM). Of particular interest are Probabilistic Finite State Automata (PFSA) (Probabilistic Finite State Machines – PFSM).

A Hidden Markov Model (HMM) [6] should be suitable for modeling the snow stages and the transitions between them, as they have been outlined above. A Markov model is a probabilistic process over a finite set, $\{S_1,..., S_k\}$, usually called its *states*. The states are not directly observable, but are related to observation X^t at time t ($t = 1, 2,..., T$) by a probability distribution of measurements,

$p(X^t | E^t = S_i)$, $i = 1, 2,..., k$,

where E^t is the unknown state of the process at time t. Thus $E^t = S_i$ indicates that the process is in state S_i at time t. The model is also described by a set of transition probabilities between each pair of states

$$p(E^t = S_i \mid E^{t-1} = S_j), \, i, j = 1, 2, ..., k.$$

Figure 4 provides state diagrams for optical and SAR observations, including legal transitions. There are probability distribution functions of time for each transition. As can be seen from the diagram, the model opens, for instance, for a transition back from snow depletion to full snow coverage. So fluctuations back and forth between two stages are allowed for a period of time, but the probability will be gradually lower as time develops into the next stage.

In order to let optical observations impose restrictions on possible SAR stages, the two models in Figure 4 have been coupled. The coupling is designed such that the state of optical observations imposes modulations to the transition probabilities between SAR observation states. The coupling will change with time, in particular being stronger as time moves into a stage (which means that the probability for SAR observations to make independent transitions then will approach zero).

VI. Discussion and conclusions

The snow coverage, as observed by optical and SAR sensors, goes through a series of stages as time moves on from winter to summer. We have here proposed a state model based on a Hidden Markov Model approach to model the observed development through the season. The model is to mitigate the typical problems when combining retrieved snow cover fraction from optical and SAR sensors using a blending approach. The model ensures that the two data sources are interpreted consistently.

The approach is currently to be implemented in various versions in order to determine the optimal model configuration. The model with the chosen configuration will then be tested on a larger dataset and compared to other published time-series multi-sensor approaches.

Acknowledgment

References

[1] T. Andersen, "Operational snow mapping by satellites," Proceedings of the Exeter symposium, July 1982, IAHS publ. no. 138, 1982, pp. 149-154.

[2] J. Koskinen, S. Metsämäki, J. Grandell, S. Jänne, L. Matikainen, and M. Hallikainen, "Snow Monitoring Using Radar and Optical Satellite Data", Remote Sensing of the Environment, vol. 69, 1999, pp. 16–29.

[3] E. Malnes and T. Guneriussen, "Mapping of snow covered area with Radarsat in Norway," Geoscience and Remote Sensing Symposium, (IGARSS), 24-28 June 2002, Vol. 1.

[4] E. Malnes, R. Storvold, R. Solberg, J. Amlien and H. Koren, "Satellite based near real-time multi-sensor retrieval of snow parameters in mountaineous areas," European Geophysical Union, Presentation in Nice, April 27, 2004.

[5] T. Nagler and H. Rott, "Retrieval of wet snow by means of multitemporal SAR data", IEEE Trans. Geoscience and Remote Sensing, Vol. 38, No. 2, March 2000, pp. 754-765.

[6] L. Rabiner "A Tutorial on Hidden Markov-Models and Selected Applications in Speech Recognition," Proceedings of the IEEE, vol. 77, no. 2, 1989, pp. 257–286.

[7] J. Raggam, A. Almer and D. Strobl, "A combination of SAR and optical line scanner imagery for stereoscopic extraction of 3-D data," Journal of Photogrammetry and Remote Sensing, vol. 49, no. 4, 1994, pp. 11-21.

[8] R. Solberg and T. Andersen, "An automatic system for operational snow-cover monitoring in the Norwegian mountain regions," Proceedings of the International Geoscience and Remote Sensing Symposium (IGARSS), 8-12 August 1994, Pasadena, California, USA, pp. 2084-2086.

[9] R. Solberg, J. Amlien, H. Koren, L. Eikvil, E. Malnes and R. Storvold (2004), "Multi-sensor and time-series approaches for monitoring of snow parameters," IEEE International Geoscience and Remote Sensing Symposium (IGARSS), Anchorage, Alaska, USA, 20-24 September 2004.

[10] R. Solberg, J. Amlien, H. Koren, L. Eikvil, E. Malnes and R. Storvold, "Multi-sensor/multi-temporal analysis of ENVISAT data for snow monitoring," ESA ENVISAT & ERS Symposium, Salzburg, Austria, 6-10 September 2004.

[11] A.B. Tait, D. K. Hall, J. L. Foster, and R. L. Armstrong, "Utilizing Multiple Datasets for Snow-Cover Mapping," Remote Sensing of the Environment, vol. 72, 2000, pp.111–126.

[12] M.L. Tampellini, P.A. Brivio, P. Carrara, D. Fantoni, S. Gnocchi, G. Ober, M. Pepe, A. Rampini, R. Ratti, F.R. Nodari and T. Strozzi, "Monitoring snow cover in alpine regions through the integration of MERIS and AATSR ENVISAT satellite observations," Proceedings of MERIS User Workshop, Frascati, Italy, 10-13 November 2003.

[13] F.T. Ulaby, R.K. Moore and A.K. Fung, Microwave Remote Sensing, Active and Passive, vol.III: From Theory to Applications, Artech House, Massachusettes, 1986.